



Spectrum of imaging findings of primary bone lymphoma in pediatric patients

Gianmarco Tuzzato¹ · Paolo Spinnato² · Giulio Vara^{3,4} · Federico Ostetto¹ · Giuseppe Bianchi¹

Received: 22 February 2024 / Revised: 18 July 2024 / Accepted: 22 July 2024
© The Author(s), under exclusive licence to Springer-Verlag GmbH Germany, part of Springer Nature 2024

Abstract

Primary bone lymphoma, a rare oncologic entity, may initially present with minimal symptoms. Presenting symptoms range from local pain and mild systemic symptoms to large palpable masses and pathologic fractures. The term “primary bone lymphoma” indicates the finding of bone involvement without other organ sites for at least 6 months. Although some radiological features may raise suspicion about this tumor form, there are no pathognomonic imaging findings, and the diagnosis will likely be delayed for a long time. The most critical radiological feature is soft tissue involvement associated with a preserved cortical layer, much more than expected for an infiltrating lesion. Anyway, very different radiological findings may be displayed in patients with primary bone lymphoma. Although these radiological features of primary bone lymphoma have been discussed in the literature by various authors, there is little data concerning imaging in pediatric patients. This paper aims to depict the possible spectrum of imaging features of primary bone lymphoma in the pediatric age, providing an exemplification pictorial essay extracted from a single institution experience in the year range period 2006–2022.

Keywords Bone neoplasms · Diagnostic imaging · Lymphoma, Non-Hodgkin · Magnetic resonance imaging · Multidetector computed tomography · Pediatrics

Introduction

Primary bone lymphoma is a rare type of cancer in children, accounting for about 5% of all primary bone cancers. It makes up less than 1% of all non-Hodgkin lymphomas and 4–5% of extra-nodal lymphomas. Only 1–2% of non-Hodgkin lymphomas in children start in the bones. Most primary bone lymphoma is diffuse large B-cell lymphomas, but there are also some rare types. Primary bone lymphoma accounts for 3–7% of all bone tumors in children, and it needs to be distinguished from more common bone tumors

such as osteosarcoma and Ewing sarcoma. It is important to suspect primary bone lymphoma in imaging tests to refer patients to specialized centers for faster diagnosis. Biopsies can often give inconclusive results, so it is crucial to have a clinical and radiological suspicion when performing them. In this article, we aim to describe the various radiological characteristics of primary bone lymphoma to help readers recognize this rare form of cancer early for better treatment options.

Clinical features

Primary bone lymphoma can occur at any age, but it is most commonly seen between the ages of 60 and 70 [1]. The femur is the most common site of occurrence, followed by the pelvis, vertebrae, and humerus. Typically, the affected area is the meta-diaphysis in the long bones [2]. Involvement of the epiphysis is considered rare [3, 4]. It is important to note that around 10–40% of cases are multifocal at onset, meaning they affect multiple areas (polyostotic) [5]. Clinically, primary bone lymphoma can be subtle, with intermittent pain as the only symptom lasting for months. Other local symptoms may include palpable swelling, while systemic

✉ Paolo Spinnato
Paolo.spinnato1982@gmail.com; paolo.spinnato@ior.it

¹ Orthopaedic Oncology Unit, IRCCS Istituto Ortopedico Rizzoli, Bologna, Italy
² Diagnostic and Interventional Radiology, IRCCS Istituto Ortopedico Rizzoli, Via GC Pupilli 1, 40136 Bologna, Italy
³ Diagnostic and Interventional Radiology, Ospedale Civile “Umberto I”, Lugo, Italy
⁴ Cellular Signalling Laboratory, Department of Biomedical and NeuroMotor Sciences (DIBINEM), University of Bologna, Bologna, Italy

symptoms may present with fever, night sweats, and weight loss. When the vertebrae are involved, it can lead to symptoms of radicular or medullary compression [5, 6].

Diagnostic criteria and imaging tools

The criterion used to establish the diagnosis of primary bone lymphoma is osseous involvement with lymphoma without accompanying extraosseous foci of involvement over a period of at least 6 months following diagnosis [7].

This form must be differentiated from the more frequent osseous metastatic non-Hodgkin lymphoma, which arises within various solid organs or lymph nodes. Radiologic findings are often non-specific and highly variable, contributing to the difficulty of timely diagnosis, as already reported by previous literature [8]. The most typical radiographic pattern is lytic-permeative bone destruction with a large transition zone. Approximately 60% of patients may additionally present with aggressive periosteal reaction. Cortical thickening and associated extra-osseous soft tissue masses are frequently seen. Suspicion could arise when a lytic lesion with poorly defined margins of the metaphysis of the long bones with aspects of periosteal reaction is identified [9]. Notably, the invasion of extra-osseous soft tissues happens even without destruction of the cortex, a distinctive aspect of round cell tumoral forms such as Ewing's sarcoma. This characteristic depends on the tumoral invasion of blood vessels that supply the bone and through which the tumor escapes outside the bone [10]. There is currently no agreement on the best way to perform imaging evaluations for children with bone lymphoma, either for assessing response

to treatment or for diagnostic purposes. This is mainly due to the rarity of the disease [11].

Conventional radiography

Conventional radiography (CR) is typically the initial imaging method used to evaluate a patient with osteoarticular pain, as recommended by the American College of Radiology (ACR) criteria for appropriateness [12].

CR may reveal certain suspicious characteristics, such as a lytic moth-eaten appearance with a wide transition zone and an aggressive periosteal reaction, most commonly of a multilamellar or “onion skin” type (Figs. 1 and 2) [13, 14]. Periosteal reactions are found in around 50–60% of primary bone lymphoma cases, usually exhibiting an aggressive pattern and more frequently occurring in long bone locations. Multiple-layer reactions are the most common (about 52% of cases), followed by single-layer reactions [15]. The radiographic approach remains valid, as it is a quick, non-invasive, and cost-effective examination.

It is important to note that this type of investigation, especially in the early stages of the disease, can yield negative findings, as primary bone lymphoma often exhibits preserved bone architecture on radiography [11]. Given the above, further radiological examination, such as magnetic resonance imaging (MRI), is recommended in cases of persistent pain associated with negative CR findings. Furthermore, it should be emphasized that other conditions, particularly Ewing's sarcoma, bone infections, and eosinophilic granuloma, may present a similar radiographic pattern. For instance, Ewing's sarcoma may arise in the diaphysis of long

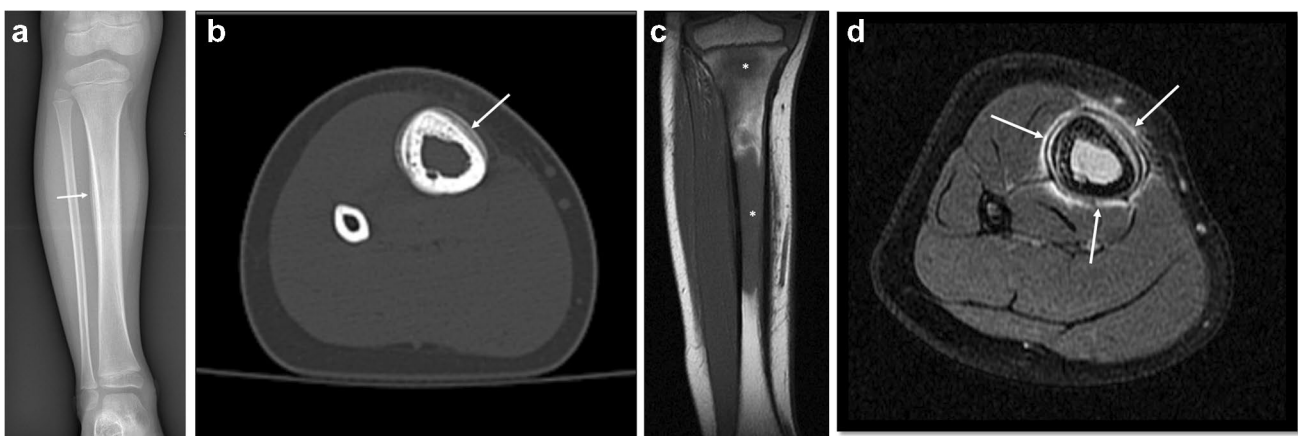
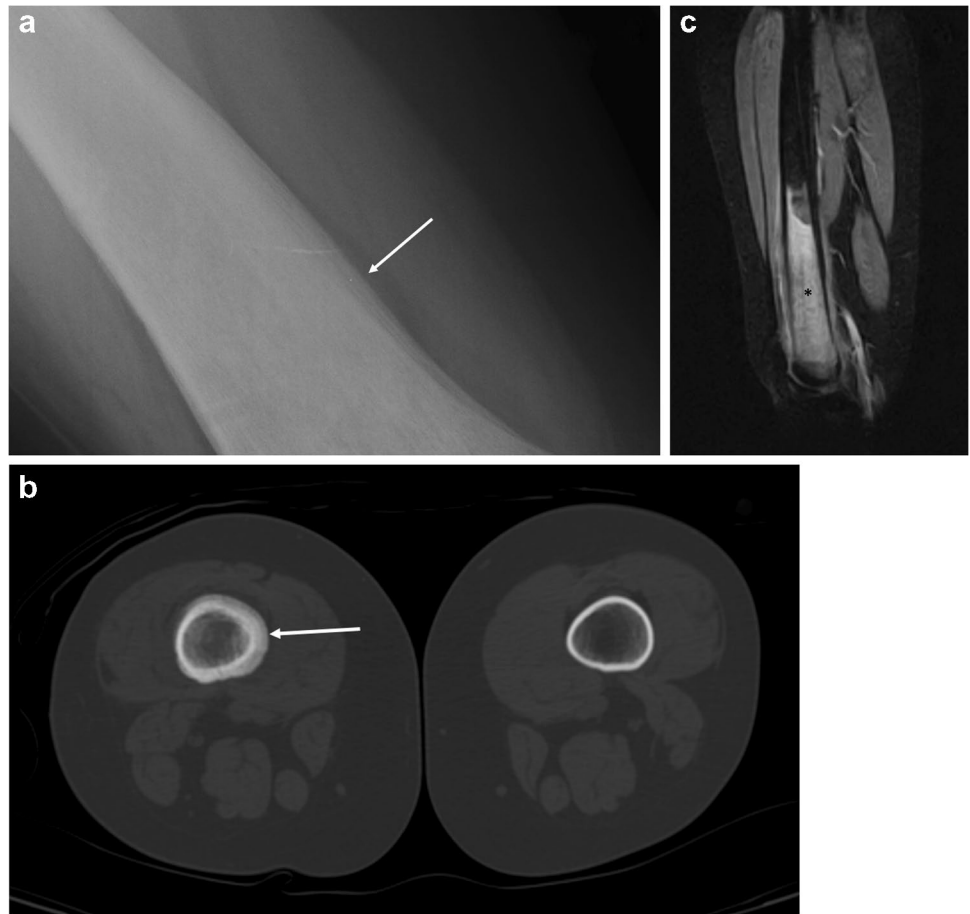


Fig. 1 **a** Conventional radiography of the leg (anteroposterior projection) of a 3-year-old girl with intermittent right leg pain for about 2 months shows a multilayered “onion skin” type of periosteal reaction on both medial and lateral aspects of the tibial shaft (*arrow*). **b** Axial computed tomography image confirms the findings in **a** (*arrow*). **c**, **d** Coronal T1W (**c**) and axial short tau inversion recovery

(**d**) magnetic resonance imaging of the leg show broad bone marrow involvement (*asterisks* in **c**) with edema of the surrounding soft tissues (*arrows* in **d**). The first minimally invasive diagnostic approach with a computed tomography-guided core-needle biopsy resulted in a non-diagnostic result. An incisional biopsy confirmed the diagnosis of non-Hodgkin B-cell bone lymphoma

Fig. 2 Images of a 13-year-old girl with dull pain in her right thigh for the preceding 3 months. **a** A magnified anteroposterior radiograph of the right femur shows a multilayered periosteal reaction “onion skin” type (*arrow*). **b** Axial computed tomography (bone windows) shows slight intramedullary sclerosis and confirms the periosteal reaction (*arrow*). **c** Sagittal T2 fat-saturated magnetic resonance image revealed a wide intramedullary bone involvement in the diaphysis and metaphysis of the distal right femur (*asterisk*). Computed tomography-guided core-needle biopsy revealed the final diagnosis of bone non-Hodgkin B-cell Lymphoma



bones with a lytic, ill-defined pattern and an extra-osseous component [16].

Computed tomography

On computed tomography (CT), primary bone lymphoma usually exhibits invasive and destructive behavior, appearing as a single lytic lesion or a set of multiple lesions (Fig. 3).

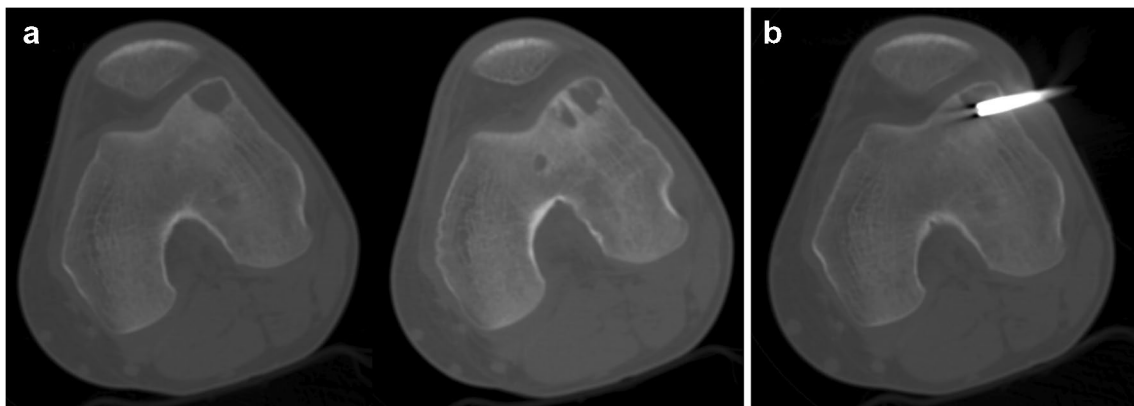


Fig. 3 Images of a 17-year-old boy with left knee pain in the preceding 2 months and a reduced range of knee flexion/extension. **a** Bone window axial computed tomography scans of the knee (upper part of the epiphysis and lower part of the epiphysis) shows a multifocal

lytic lesion, with sharp perilesional sclerosis. **b** Computed tomography-guided core-needle biopsy performed within the lesion with an 8-gauge trap-system needle revealed the diagnosis of non-Hodgkin B-cell bone lymphoma

CT can also demonstrate the presence of cases in which lytic and sclerotic patterns coexist.

Sclerotic changes are more commonly seen in the spine than in the appendicular skeleton (Fig. 4) [17]. It is important to note that sclerotic changes are frequently observed as a response to drug therapies [18]. A CT scan can also detect periosteal reactions, which are present in more than half of patients. Although there are no definitive features on CT, strong diagnostic suspicion arises when a bone lesion involving extra-osseous soft tissues is identified, with minimal or no destruction of the cortical bone (Fig. 5). Dual-energy CT technology may aid in characterizing bone lesions [19]. However, in pediatric patients, this technology may be less

useful due to the high water content of red bone marrow, resulting in lower sensitivity for identifying primary bone lymphoma lesions.

According to the American College of Radiology (ACR), CT scans are primarily useful for guiding biopsies or for conducting total body scans to rule out other disease locations [12].

Magnetic resonance imaging

MRI is the most sensitive imaging tool for the assessment of suspect or confirmed primary bone lymphoma. MRI appears to be a fundamental examination for diagnosing primary

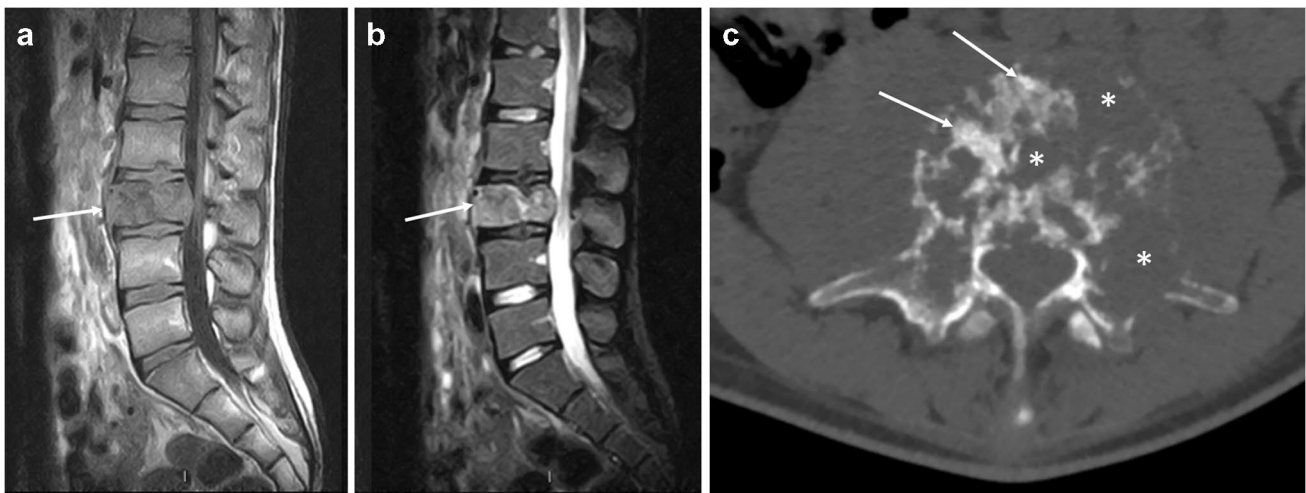


Fig. 4 Images of a 16-year-old boy with severe low-back pain which started 3 months before, non-responsive to analgesic drugs. Intermittent fever was also present. **a**, **b** Sagittal T1 (**a**) and T2 (**b**) magnetic resonance imaging sagittal T1w of the spine reveal a pathological fracture (*arrows*) with an intracanal protrusion of the posterior wall of the vertebral body. **c** Axial spinal computed

tomography image (bone windows) shows both lytic (*asterisks*) and sclerotic (*arrows*) areas present in the body of L3. Wide cortical disruptions with several lytic foci are detectable. An extra-osseous component in the right psoas region is present. Computed tomography-guided core-needle biopsy revealed the diagnosis of non-Hodgkin B-cell bone lymphoma



Fig. 5 Images of a 10-year-old boy with left hip pain worsening during physical activities. **a** Anteroposterior conventional radiography of the pelvis shows a disruptive lytic lesion with ill-defined margins of the left iliac wing involving the anterior superior iliac tuberosity (*arrow*). **b** Axial computed tomography of the pelvis with bone

window and contrast-enhanced soft-tissue window confirm the presence of a lytic lesion of the left iliac wing with cortical disruption (*arrow* in **b**) and soft-tissue extra-osseous components (*asterisks* in **c**). **c** Computed tomography-guided core-needle biopsy revealed the diagnosis of non-Hodgkin B-cell bone lymphoma

bone lymphoma and its follow-up; this method makes it easy to identify a replacement process of the normal bone marrow, the involvement of the peripheral soft tissues, and the permeated aspect at the cortical level (Fig. 6) [11, 20]. In patients with primary bone lymphoma, T1-weighted sequences show areas of low intensity and are suitable for identifying changes in the bone marrow. Similarly, the same areas in T2-weighted sequences with the fat-saturation technique show a high or intermediate signal intensity. The administration of contrast medium shows varying uptake patterns, particularly an infarct-like enhancement pattern that has been recently described in pediatric primary bone lymphoma (Fig. 7) [11]. Nonetheless, MRI appears to be a fundamental examination for defining the involvement of periskeletal soft tissues.

Considering the high hematopoietic content of the bone marrow in children, it could be difficult to differentiate active hematopoietic bone marrow from pathologic conditions, particularly into the very active marrow areas, depending on the patient's age; in this regard, a recent research by Tonkaz et al. revealed that the addition of out-of-phase/in-phase signal ratio together with fat fraction can help in differentiating between malignant and benign condition [21].

Lastly, it has been demonstrated that DWI sequences on MRI are more specific than traditional MRI methods [22]; anyway, for primary bone lymphoma, the degree of

restricted diffusivity is not as pronounced as other types of lymphoma, and diffusion restriction is not specific to primary bone lymphoma. While extra-nodal musculoskeletal soft tissue lymphomas present with a well-recognizable and constant radiological presentation (homogeneous on MRI, infiltrative, without necrosis, fat, or fibrosis), on the contrary, primary bone lymphoma can display a wide range of different features (sclerotic, lytic, ill-defined or well-defined margins) [11, 23]. In a study with adult patients affected by bone lymphoma, a mean apparent diffusion coefficient (ADC) was used to identify the bone marrow involvement with a cutoff value of 0.498 for focal and 0.401 for diffuse bone involvement [24].

Whole-body MRI (DWI sequences) showed an excellent concordance with FDG PET-CT in assessing lymphoma bone marrow involvement; due to this and also to the absence of ionizing radiation, whole-body MRI could play a key role in assessing primary bone lymphoma, especially in pediatric patients [25].

Positron emission tomography (PET)

The PET scan shows excellent sensitivity in patients with primary bone lymphoma as this type of lesion has a high fluorodeoxyglucose uptake, despite a low specificity (Fig. 8) [26].

Fig. 6 Images of a 17-year-old girl patient with spontaneous shoulder pain in the preceding 4 months and fever since the last few weeks. Magnetic resonance imaging of the shoulder, coronal T1w (a), T2w fat sat (b), and computed tomography of the shoulder with 3D reconstruction (c), and coronal view (d) show an osteolytic lesion with thin-focal cortical disruption (arrows) as well as extraosseous involvement (asterisks) of proximal metaphysis of the left humerus. The histological report, obtained via computed tomography-guided core-needle biopsy, confirmed the diagnosis of non-Hodgkin B-cell bone lymphoma

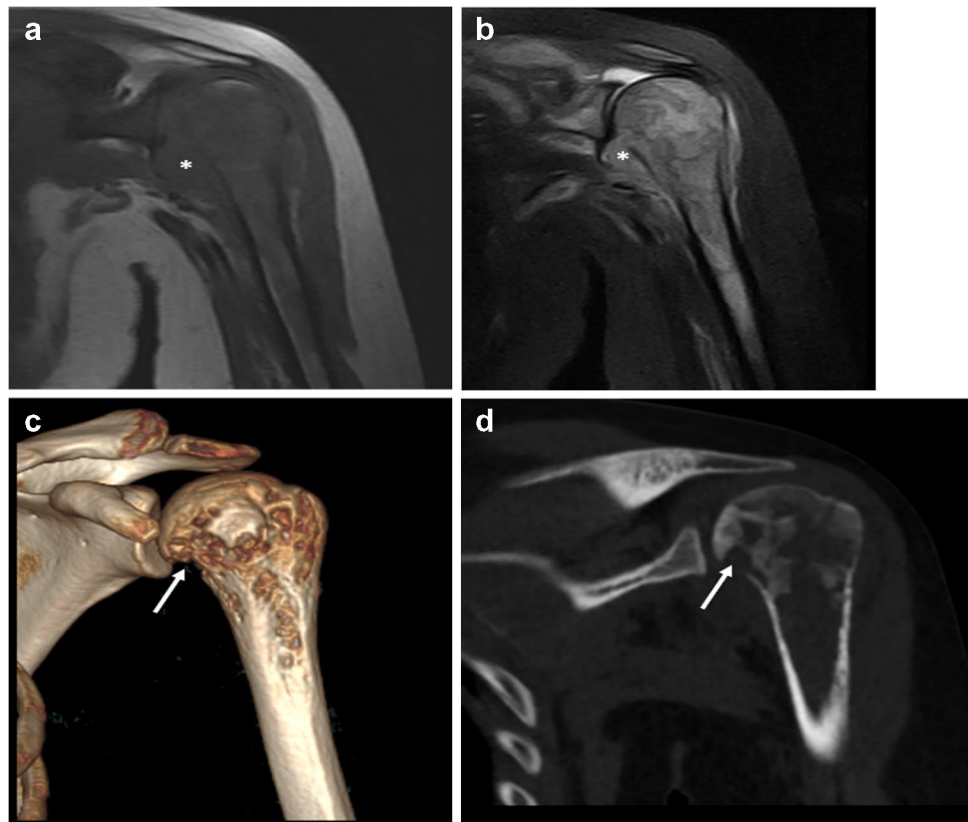


Fig. 7 Computed tomography (CT) and magnetic resonance imaging (MRI) of the knee of a 14-year-old boy with continuous right knee pain in the last 4 months and intermittent fever. Coronal CT view (a) shows mild diffuse sclerosis of the proximal tibia with a central area referable to osteonecrosis (arrow). MRI T1w coronal view (b) and T1w contrast-enhanced sagittal (c) show multiple foci of bone marrow infiltration in the epiphysis and metaphysis of the tibia and the metaphysis of the distal femur (arrows). An infarct-like enhancement pattern can be noted in the proximal tibia (c, asterisks). The follow-up knee MRI control sagittal T1w (d) after therapies (1 year later) shows a complete normalization of bone marrow signal intensity in both femur and tibia and a significant increase of multiple osteonecrosis areas involving both the femur and tibia (asterisks)



In a previous study on adult patients, the standard uptake value max-ratio-cutoff value was 95.25% for focal and 70.2% for diffuse bone marrow involvement.

At diagnosis, PET-CT is useful for staging, allowing the identification of other possible sites of disease. During follow-up, PET, more than MRI and CT, helps define the disease's response to drug treatments, indicating post-therapeutic changes, including necrosis and fibrosis [26].

When compared to 18F-FDG PET or MRI alone, integrated whole-body 18F-FDG PET/MRI demonstrated superior sensitivity and accuracy in identifying body mass index in indolent lymphoma, indicating that 18F-FDG PET/MRI is a dependable substitute for bone marrow biopsy [27].

Anatomical sites of skeletal lesions

The femur is usually reported as the most commonly affected skeletal site for primary bone lymphoma lesions. Regarding the intra-osseous location of lesions, metaphyses are the most frequently involved skeletal regions. A few previous literature data revealed that even the epiphysis of long bones could also commonly be affected (Fig. 9) [10, 20]. However, we remark that all skeletal regions may be affected by primary bone lymphoma, sometimes rendering its initial diagnosis even more difficult (Fig. 10).

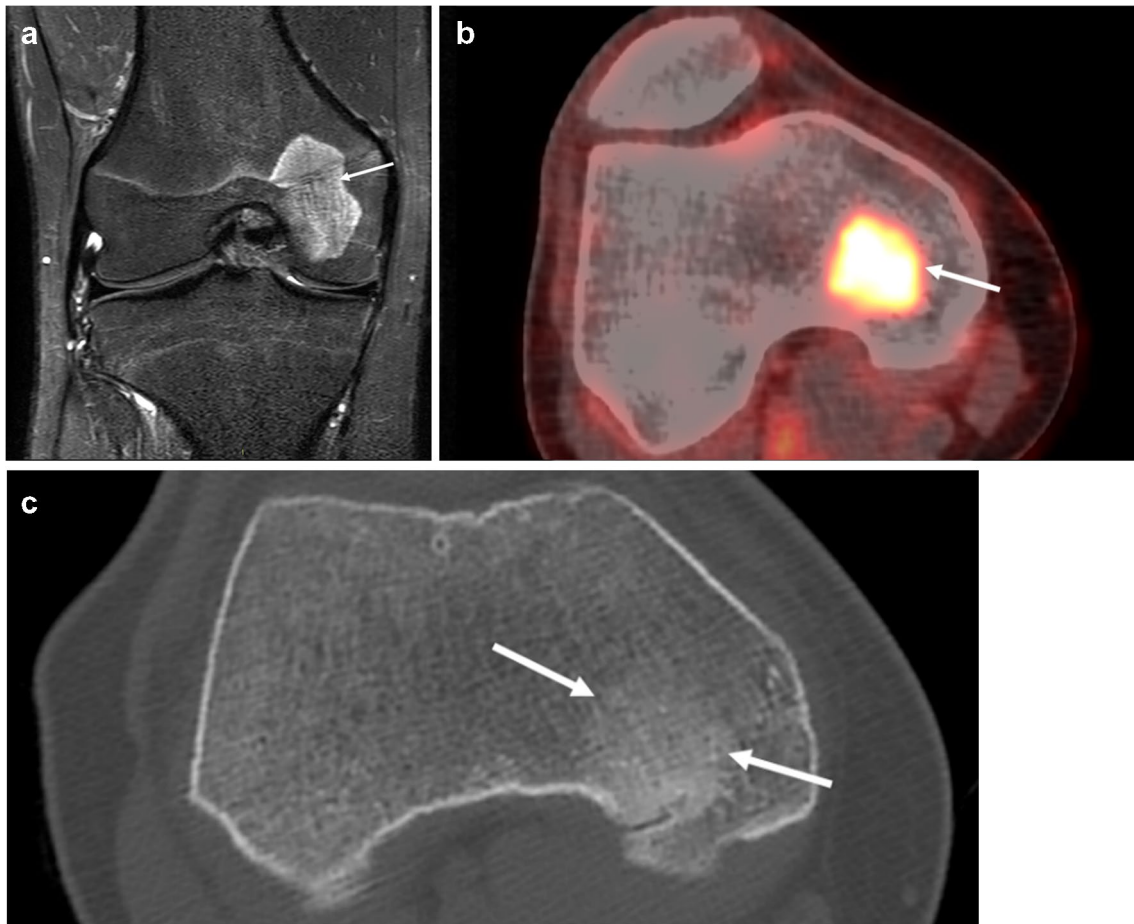


Fig. 8 Images of a 13-year-old boy with an asymptomatic focal bone lesion incidentally detected on a knee magnetic resonance imaging (MRI) performed after a sprain injury of the knee. A well-defined lesion on the distal epiphysis of the right femur (*arrow*) is displayed on MRI coronal view of the knee T2w fat saturated (**a**). Positron

emission tomography-computed tomography (**b**) shows high fluoro-deoxyglucose uptake (standard uptake value max=6), and computed tomography (**c**) shows a sclerotic pattern (*arrows*). A computed tomography-guided core-needle biopsy revealed the diagnosis of non-Hodgkin B-cell bone lymphoma

Conclusion

Our collection of images of pediatric patients with primary bone lymphoma shows a wide range of different imaging features. Unlike extra-nodal musculoskeletal soft tissue lymphomas, which have consistent MRI findings (homogeneous, infiltrative, without necrosis, fat, or fibrosis), primary bone lymphoma can display various features such as sclerotic, lytic, and ill-defined or well-defined margins. The most common radiological pattern is an ill-defined, lytic focal bone lesion, often with extraosseous components and a periosteal reaction (usually “onion skin” type). However, a purely sclerotic pattern may also be seen. These findings are consistent with previous cases reported.

These features can also be seen in other conditions such as Ewing’s sarcoma and bone infections. Ewing’s sarcoma, for example, may present with a lytic ill-defined

pattern and an extra-osseous component. Primary bone lymphoma can have different presentations, which can complicate the differential diagnosis.

The onset is also extremely wide, associated with fleeting and non-specific symptoms. The diagnosis of primary bone lymphoma can be challenging because it can resemble other conditions. While X-rays are often the first step in imaging, they may not always provide a clear diagnosis for symptomatic patients. Therefore, more specific and sensitive diagnostic studies are needed for patients with inconclusive X-ray results. In conclusion, while imaging plays an essential role in identifying potential issues, it should prompt further specific diagnostic studies through tissue sampling at specialized centers. This approach aims to facilitate a prompt and accurate diagnosis, enabling the development of tailored treatment strategies.

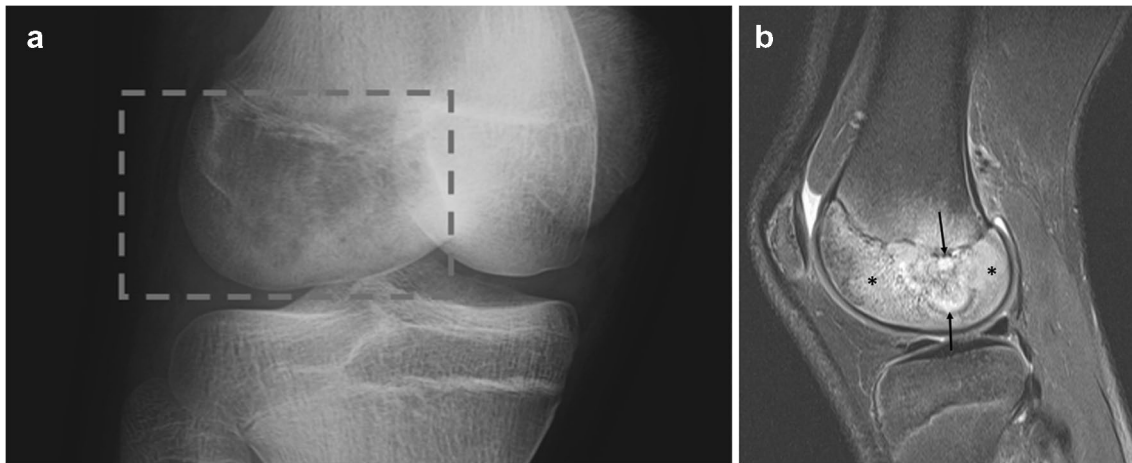


Fig. 9 Images of a 14-year-old boy with continuous right knee pain in the preceding 3 months, increasing during weight bearing. Magnification of conventional radiography, anteroposterior-oblique view, of the right knee (**a**), shows a lytic lesion at the distal epiphysis of the femur (lateral condyle, *dotted square*) with ill-defined margins.

MRI (**b**) confirms the lesion located in the distal epiphysis (*arrows*) surrounded by wide bone marrow edema involving the whole lateral condyle (*asterisks*). A computed tomography-guided core-needle biopsy resulted to be inconclusive. A subsequent surgical incisional biopsy revealed the diagnosis of non-Hodgkin B-cell bone lymphoma

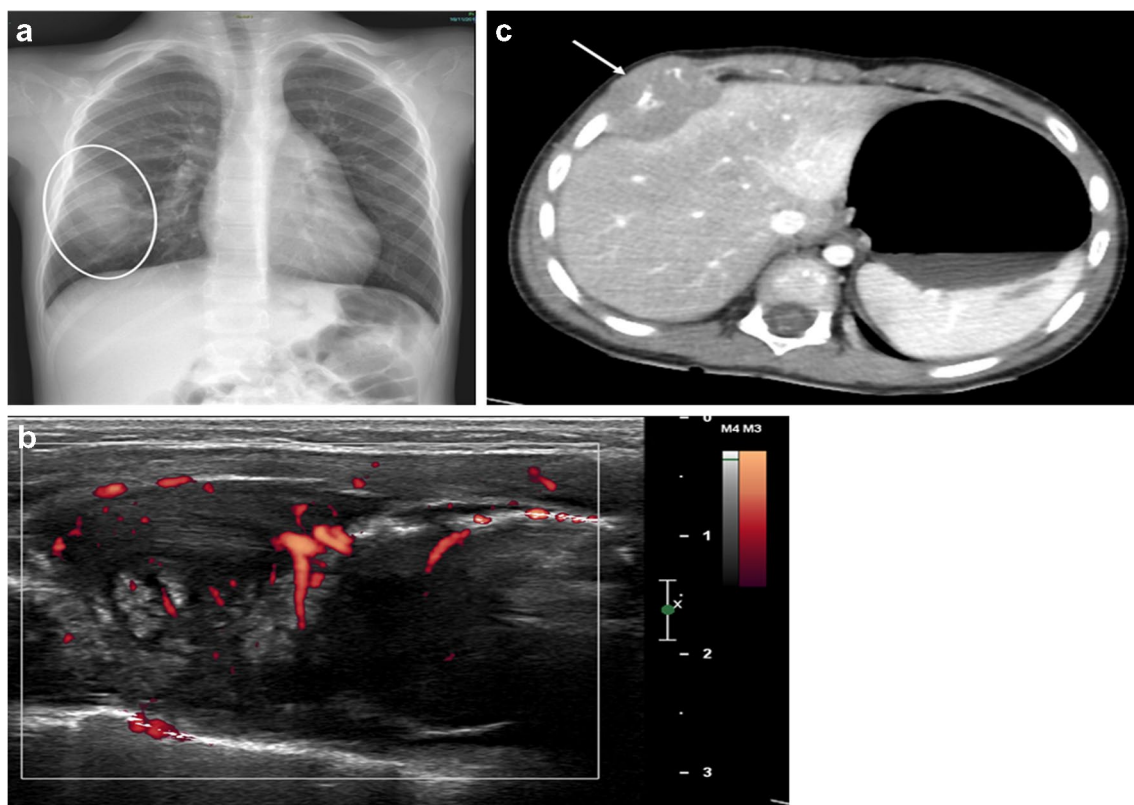


Fig. 10 Images of a 5-year-old boy with chest pain and palpable mass at the right lower anterior chest wall. Chest X-rays, posteroanterior view (**a**) shows a thoracic radio-opacity (*oval line*) involving the anterior arch of the fifth right rib. Ultrasound with power Doppler shows an inhomogeneous neoplasm with rich internal vascularization (**b**).

Contrast-enhanced computed tomography confirms the presence of a lytic lesion involving the fifth right rib and a wide extraosseous soft tissue component (**c**, *arrow*). A computed tomography-guided core-needle biopsy revealed the diagnosis of non-Hodgkin B-cell bone lymphoma

Acknowledgements We thank Roberta Laranga (data manager at IRCCS Istituto Ortopedico Rizzoli, Bologna, Italy) for helping with the formal analysis of this paper.

Author contribution Conceptualization P.S., writing P.S. and G.T., supervision G.B., data curation F.O., software P.S., G.V., and G.T., writing reviewing and editing P.S., G.B., and G.T., literature analysis G.V., F.O., and G.T., data collection P.S., G.T., and F.O. All the authors approved the final version of the manuscript.

Data availability Additional data or further information can be requested by mail to the corresponding author.

Declarations

Ethics approval We declare that this research does not involve human and/or animals participants.

Conflicts of interest None

References

- Huebner-Chan D, Fernandes B, Yang G, Lim MS (2001) An immunophenotypic and molecular study of primary large B-cell lymphoma of bone. *Modern Pathol* 14:1000–1007
- Bhagavathi S, Micale MA, Les K et al (2009) Primary bone diffuse large B-cell lymphoma: clinicopathologic study of 21 cases and review of literature. *Am J Surg Pathol* 33:1463–1469
- Fox MG, Marti JK, Bachmann KR et al (2015) Epiphyseal presentation of non-Hodgkin's lymphoma of bone in two pediatric patients—one with primary lymphoma of bone. *Skeletal Radiol* 44:587–595
- Yan JJ, Chou AJ, Giulino-Roth L, Pomeranz CB (2024) Pediatric primary lymphoma of bone in epiphysis case report. *Skeletal Radiol* 53:401–406
- Binici DNR, Karaman A, Timur O et al (2018) Primary skeletal muscle lymphoma: a case report. *Mol Clin Oncol* 8:80–82
- de Camargo OP, dos Santos Machado TM, Croci AT et al (2002) Primary bone lymphoma in 24 patients treated between 1955 and 1999. *Clin Orthop Relat Res* 397:271–280
- Ebus SC, Bernsen HJ, Norel Van GJ, Donk R (2002) Primary non-Hodgkin's lymphoma in multiple vertebrae presenting as a lumbar radicular syndrome: a case report. *Spine* 27:E271–E273
- Milks KS, McLean TW, Anthony EY (2016) Imaging of primary pediatric lymphoma of bone. *Pediatr Radiol* 46:1150–1157
- McCormack LJ, Ivins JC, Dahlin DC, Johnson EW Jr (1952) Primary reticulum-cell sarcoma of bone. *Cancer* 5:1182–1192
- Ben Abdelghani K, Rouached L, Mourad Dali K et al (2021) Diffuse large B cell lymphoma presenting with renal failure and bone lesions in a 46-year-old woman: a case report and review of literature. *CEN Case Rep* 10:165–171
- Duffy P, Ecklund K (2023) MR features of primary bone lymphoma in children. *Pediatr Radiol* 53:2400–2410
- Expert Panel on Musculoskeletal Imaging, Bestic JM, Wessell DE et al (2020) ACR Appropriateness Criteria® primary bone tumors. *J Am Coll Radiol: JACR* 17:S226–S238
- Krishnan A, Shirkhoda A, Tehranzadeh J et al (2003) Primary bone lymphoma: radiographic-MR imaging correlation. *Radiographics* 23:1371–1387
- Rana RS, Wu JS, Eisenberg RL (2009) Periosteal reaction. *AJR Am J Roentgenol* 193:W259–W272
- Mulligan ME, McRae GA, Murphey MD (1999) Imaging features of primary lymphoma of bone. *AJR Am J Roentgenol* 173:1691–1697
- Weber MA, Papakonstantinou O, Nikodinovska VV, Vanhoenacker FM (2019) Ewing's sarcoma and primary osseous lymphoma: spectrum of imaging appearances. *Semin Musculoskelet Radiol* 23:36–57
- Messina C, Christie D, Zucca E et al (2015) Primary and secondary bone lymphomas. *Cancer Treat Rev* 41:235–246
- Braun RA, Milito CF, Goldman SM, Fernandes Ede Á (2016) Ivory vertebra: imaging findings in different diagnoses. *Radiol Bras.* 49:117–21
- Burke MC, Garg A, Youngner JM et al (2019) Initial experience with dual-energy computed tomography-guided bone biopsies of bone lesions that are occult on monoenergetic CT. *Skeletal Radiol* 48:605–613
- Navarro SM, Matcuk GR, Patel DB (2017) Musculoskeletal imaging findings of hematologic malignancies. *Radiographics* 37:881–900
- Erkal Tonkaz D, Ozpar R, Tonkaz M, Yazici Z (2024) Efficacy of fat quantification methods used in MRI to distinguish between normal, benign, and malignant bone marrow pathologies in children. *Acta Radiologica (Stockholm, Sweden : 1987)*, 2841851241247110. Advance online publication. <https://doi.org/10.1177/02841851241247110>
- Jiang XX, Yan ZX, Song YY, Zhao WL (2013) A pooled analysis of MRI in the detection of bone marrow infiltration in patients with malignant lymphoma. *Clin Radiol* 68:e143–e153
- Spinnato P, Chiesa AM, Ledoux P et al (2023) Primary soft-tissue lymphomas: MRI features help discriminate from other soft-tissue tumors. *Acad Radiol* 30:285–299
- Asenbaum U, Nolz R, Karanikas G et al (2018) Bone marrow involvement in malignant lymphoma: evaluation of quantitative PET and MRI biomarkers. *Acad Radiol* 25:453–460
- Balbo-Mussetto A, Saviolo C, Fornari A et al (2017) Whole body MRI with qualitative and quantitative analysis of DWI for assessment of bone marrow involvement in lymphoma. *Radiol Med (Torino)* 122:623–632
- Pu Y, Wang C, Xie R et al (2023) Role of 18F-fluorodeoxyglucose PET/computed tomography in the diagnosis and treatment response assessment of primary bone lymphoma. *Nucl Med Commun* 44:318–329
- Chen X, Yuan T, Wei M et al (2023) Diagnostic performance of integrated whole-body ¹⁸F-FDG PET/MRI for detecting bone marrow involvement in indolent lymphoma: comparison with ¹⁸F-FDG PET or MRI alone. *Front Oncol* 13:1136687

Publisher's Note Springer Nature remains neutral with regard to jurisdictional claims in published maps and institutional affiliations.

We declare that this research is original and has been submitted solely to "Pediatric Radiology."

Springer Nature or its licensor (e.g. a society or other partner) holds exclusive rights to this article under a publishing agreement with the author(s) or other rightsholder(s); author self-archiving of the accepted manuscript version of this article is solely governed by the terms of such publishing agreement and applicable law.